

## Zinc-induced modification of the dynamical magnetic susceptibility in the superconducting state of $\text{YBa}_2\text{Cu}_3\text{O}_{6+x}$ as revealed by inelastic neutron scattering

Y. Sidis, P. Bourges, and B. Hennion

*Laboratoire Léon Brillouin, CEA-CNRS, Centre d'Etudes de Saclay, 91191 Gif-sur-Yvette, France*

L. P. Regnault

*Centre d'Etudes Nucléaires de Grenoble, Département de Recherche Fondamentale sur la Matière Condensée, Service de Physique Statistique, Magnétisme et Supraconductivité, Groupe Magnétisme et Diffraction Neutronique, 85 X, 38041 Grenoble cedex, France*

R. Villeneuve and G. Collin

*Laboratoire Léon Brillouin, CEA-CNRS, Centre d'Etudes de Saclay, 91191 Gif-sur-Yvette, France*

J. F. Marucco

*Laboratoire des Composés Non-Stoechiométriques, CNRS URA 446, Bâtiment 415, Université Paris Sud centre d'Orsay, Orsay, France*

(Received 30 March 1995; revised manuscript received 6 July 1995)

Inelastic-neutron-scattering measurements have been performed to determine the imaginary part of the dynamical susceptibility,  $\chi''(Q, \omega)$ , of a  $\text{YBa}_2(\text{Cu}_{1-y}\text{Zn}_y)_3\text{O}_{6.97}$  sample exhibiting a superconducting transition at  $T_c=69$  K. Zinc substitution induces striking modifications of the energy dependence of  $\chi''(Q, \omega)$  but magnetic fluctuations remain peaked at the antiferromagnetic wave vector,  $Q_{\text{AF}}$ , at all investigated energies. In the superconducting state of the zinc-free compound,  $\chi''(Q, \omega)$  is restricted to a narrow energy range,  $\hbar\omega=33-47$  meV, displaying a *spin gap* at  $E_G=33$  meV and a resonant enhancement at  $E_r=39$  meV, both features vanishing upon heating up above  $T_c$ . In the  $y=0.02$  substituted sample in the superconducting state, there is still an energy band in the range 32–47 meV but no clear resonance, and a signal is now observed in the low energy range, though the line shape of  $\chi''(Q, \omega)$  indicates some reminiscence of the spin gap of the pure compound.

### I. INTRODUCTION

In the present paper, we consider the substitution of a copper ion by a zinc ion in  $\text{CuO}_2$  planes in  $\text{YBa}_2\text{Cu}_3\text{O}_{6+x}$  (YBCO) compound, which is known to strongly reduce the superconducting transition temperature,  $T_c$ ,<sup>1</sup> with only a negligible variation of the charge transfer.<sup>2</sup> Since Zn has a closed-shell  $3d^{10}$  configuration, this strong effect on superconductivity is striking. Indeed, in terms of conventional superconductivity, the role of such a nonmagnetic impurity should be minor.<sup>3</sup> This quite unusual effect is a hint that the substitution affects the mechanism of the high- $T_c$  superconductivity. Consequently, the zinc dependence of the superconducting properties could provide valuable information in the understanding of the nature of the superconductivity.

In high- $T_c$  cuprates, the persistence of antiferromagnetic (AF) fluctuations in the metallic state is probably one of the most striking features. In the superconducting state of  $\text{YBa}_2\text{Cu}_3\text{O}_{6+x}$  compounds, previous inelastic-neutron-scattering (INS) studies have established the existence of an energy gap in the imaginary part of the dynamical magnetic susceptibility,  $\chi''(Q, \omega)$ . Below this characteristic energy  $E_G$ , the so-called *spin gap*, no intensity can be found up to  $T_c$ .<sup>4,5</sup> INS results have also shown that  $\chi''(Q_{\text{AF}}, \omega)$  is characterized by a strong enhancement of the intensity, almost energy resolution limited, at some energy  $E_r$ . This resonance feature exhibits a smaller  $Q$  width than the magnetic response at other energies and appears to be strongly correlated

to the superconductivity, as shown by its temperature dependence.<sup>4-6</sup> The resonance, which is unambiguously established for an oxygen content larger than  $x \approx 0.8$ , becomes more and more pronounced with increasing hole doping. Several theories, among which a large number has been developed in the framework of the  $t-t'-J$  model,<sup>7</sup> may account for these features, but the implication of these properties as regards the mechanism of superconductivity is still highly debated. Thus zinc substitution could be viewed as a way to probe how closely related are magnetism and superconductivity in cuprates.

Up to now, INS measurements on zinc substituted YBCO have only investigated nonsuperconducting states,<sup>8,9</sup> or superconducting samples exhibiting a  $T_c$  too small ( $\approx 10$  K) to probe accurately how zinc substitution affects the magnetic properties in the superconducting state.<sup>10</sup> Due to the availability of a sufficiently large single crystal of  $\text{YBa}_2(\text{Cu}_{1-y}\text{Zn}_y)_3\text{O}_{6.97}$ , we have performed INS measurements in the superconducting state in order to characterize how  $\chi''(Q, \omega)$ , and more precisely, the spin gap and the resonance feature behave under zinc substitution.

The paper is organized as follows: Sec. II is devoted to the description of the sample and of the experimental conditions. The next two sections are concerned with the description and analysis of the experimental results; in Sec. III we present evidence of low energy correlated magnetic response below and above  $T_c$  and in Sec. IV we focus on the drastic evolution of the resonance feature. A detailed comparison

with the magnetic response of the pure system is presented in Sec. V. The results of our INS study are related to results obtained by other techniques and some conclusions about the way that zinc substitution induces such drastic changes in the superconducting properties of YBCO are presented in Sec. VI.

## II. SAMPLE PREPARATION AND EXPERIMENTAL CONDITIONS

The  $\text{YBa}_2(\text{Cu}_{1-y}\text{Zn}_y)_3\text{O}_{6+x}$  single crystal was grown by flux method giving a mosaic spread of  $2.2^\circ$  and a volume of  $0.2\text{ cm}^3$ . The sample was prepared in the fully oxidized state, after heat treatment (five days at  $300^\circ\text{C}$ ). The zinc content has been established by measuring the superconducting transition temperature,  $T_c$ , which was found to be  $69\text{ K}$ , yielding a zinc content of  $y=2\%$ .<sup>1</sup> This sample, reduced to  $\text{O}_{6.1}$ , exhibits a three-dimensional (3D) antiferromagnetic order with a Néel temperature,  $T_N=355\text{ K}$ .<sup>11</sup> At room temperature, the  $c$  lattice parameter is  $11.671(4)\text{ \AA}$ , yielding an oxygen content  $x=0.97\pm 0.03$ . Therefore, the sample belongs to the overdoped regime<sup>4,5</sup> and all the results will be compared with those of  $\text{YBa}_2\text{Cu}_3\text{O}_{6.97}$  ( $T_c=92.5\text{ K}$ ).<sup>12</sup>

INS experiments were carried out on the  $2T$  triple-axis spectrometer installed on a thermal beam at the Orphée reactor in Saclay. Pyrolytic graphite (PG002) or copper (Cu111) crystals have been used as monochromators and a PG002 as analyzer. In order to get the maximum scattered intensity, monochromators and analyzer were bent horizontally and vertically.<sup>13</sup> Measurements have been performed with a final wave vector of  $4.1\text{ \AA}^{-1}$ . Pyrolytic graphite filter was put in the scattered beam, to remove higher order contamination. To benefit from the focusing effects of both analyzer and monochromators, no slit collimators were used in a way similar to our previous YBCO studies.<sup>4,5,9,12</sup> The sample, aligned with the (110) and (001) directions in the scattering plane, was fixed to the cold finger of a displex refrigerator system. These experimental conditions were strictly the same as those used for the measurements on the pure YBCO. In order to get a direct comparison of the intensities scattered by pure and zinc substituted samples, a longitudinal phonon has been measured in both samples (Fig. 1). This yielded a scaling factor of 3, very near the ratio of the samples weights.

Finally, before presenting the experimental results, let us briefly recall that one of the specific characteristics of YBCO is the  $\text{CuO}_2$ -bilayer structure. This results in a magnetic structure factor exhibiting maxima along the AF rod  $Q_{\text{AF}}=(0.5, 0.5, q_1)$  for  $q_1\approx 1.6$  and  $5.2$ . This structure factor is combined with the magnetic form factor of Cu and the maximum magnetic intensity is expected at  $q_1\approx 1.6$ . Unfortunately this value restricts the accessible energy range to  $\hbar\omega < 20\text{ meV}$ . The measurements in this energy range, herein after referred to as the low energy study, are presented in Sec. III. To access higher energies we had to perform measurements around  $q_1\approx 5.2$ . The results, referred to as the high energy study, are presented in Sec. IV.

## III. LOW ENERGY STUDY

To investigate the effect of zinc substitution on  $\chi''(Q, \omega)$  at low energy, we have performed  $Q$  scans across the magnetic

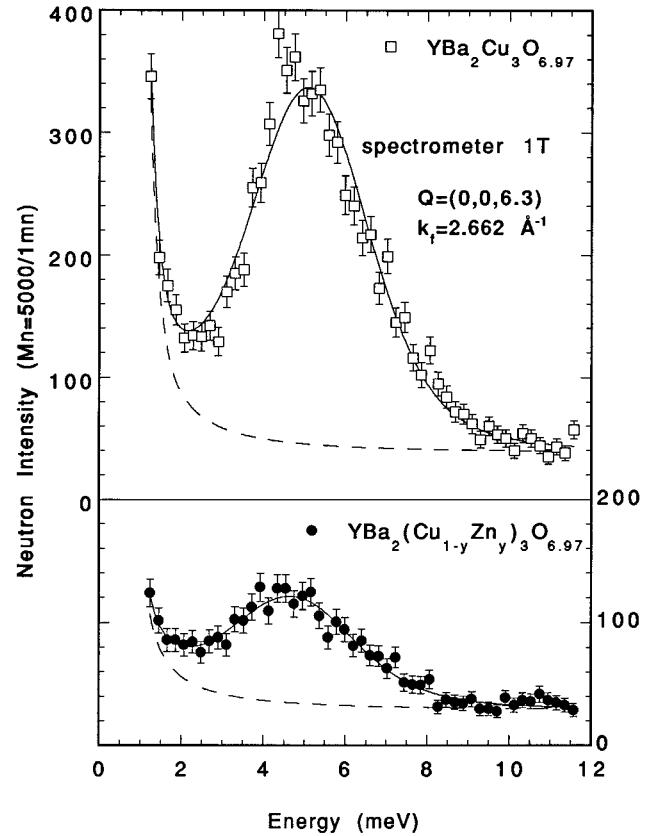


FIG. 1. Longitudinal acoustic phonon along the  $c$  axis, measured at room temperature in  $\text{YBa}_2\text{Cu}_3\text{O}_{6.97}$  (open squares) and  $\text{YBa}_2(\text{Cu}_{1-y}\text{Zn}_y)_3\text{O}_{6.97}$  (full circles) and used to scale the magnetic intensities. Full lines result from a fit using a damped harmonic oscillator convoluted with the resolution function on top of a background (dashed lines). The small apparent shift could result from a small change of the lattice dynamics due to zinc substitution, but it is more likely an artifact due to an asymmetric line shape, non-accounted for by the fit, and more obvious with the higher counting rate.

rod [hereafter: “in the (110) direction”] around the scattering wave vector  $Q_{\text{AF}}=(0.5, 0.5, 1.6)$  for an energy  $\hbar\omega=10\text{ meV}$  using the PG002 monochromator. Such a measurement, performed at  $T=10.5\text{ K}$ , exhibits a clear correlated intensity around  $Q_{\text{AF}}$  [Fig. 2(a)]. The shape of the background is very similar to that observed in the zinc-free sample at  $T=4.5\text{ K}$  for the same energy [also reported in Fig. 2(a)], where no signal was observed. The experimental data have been analyzed using a Gaussian response in addition to a “parabolic” background. In Fig. 2(a), the full line results from the best fit using such an analysis with  $\Delta Q=0.16\pm 0.02\text{ r.l.u.}$ , which yields  $\Delta Q\approx 0.29\text{ \AA}^{-1}$  after simple Gaussian deconvolution of the instrumental resolution function.

In order to probe the magnetic nature of the correlated intensity, we have performed a  $q_1$  scan along the magnetic rod. As mentioned above, the “acoustic” structure factor of magnetic fluctuations should obey the relation  $S(Q, \omega)\propto f^2(Q)\sin^2(\pi z q_1)$ , where  $z=0.291$  is the reduced distance between Cu nearest neighbors within a bilayer, and  $f(Q)$  is the copper magnetic form factor. In Fig. 2(b), the full line displays such a structure factor on top of a parabolic

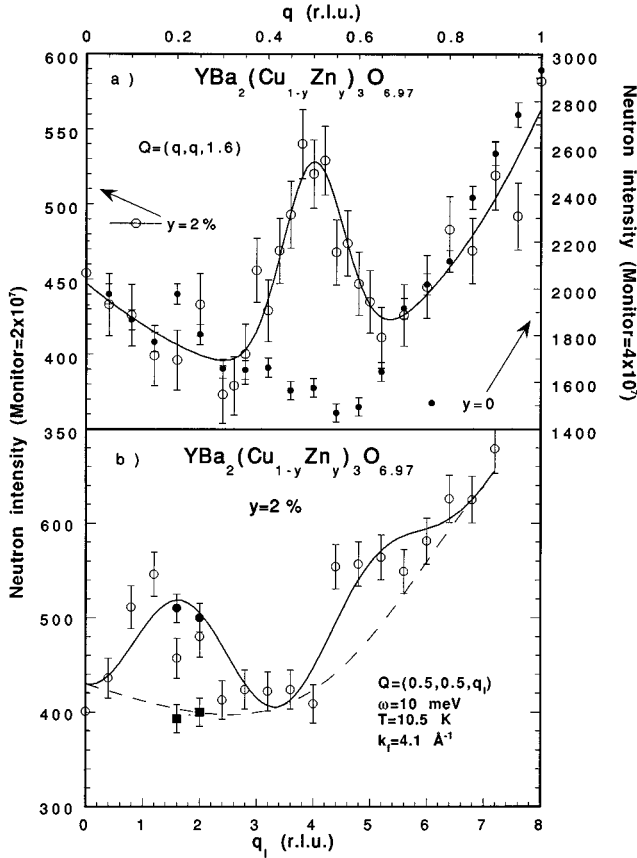


FIG. 2. (a)  $Q$  scan across the magnetic rod at  $q_1=1.6$  and at  $\hbar\omega=10$  meV, with the PG002 monochromator: at  $T=10.5$  K, our results on zinc substituted sample (open circles, left scale), and at  $T=4.5$  K, those on the zinc-free sample of Ref. 12 (closed circles, right scale). (b)  $Q_1$  scan performed at  $Q_{AF}$  along the (001) direction at  $\hbar\omega=10$  meV and  $T=10.5$  K (open circles). Full symbols correspond to the analysis of additional  $Q$  scans across the magnetic rod yielding maximum intensity (circle) and background (square). The solid line corresponds to the “acoustic” structure factor of the magnetic fluctuations on top of a parabolic background (dashed line).

background, which establishes the magnetic nature of this intensity.

To get more information on the energy dependence of  $\chi''$ , we performed an energy scan at  $Q=(0.5, 0.5, 1.6)$  at  $T=10.5$  K. In order to separate the correlated magnetic contribution from the background, several  $Q$  scans have been performed in the direction (110) and analyzed with a Gaussian line shape. The results are reported on Fig. 3(a), where the open circles are the energy scan values, full circles and squares are the fitted values, respectively, for signal and background, obtained from the analysis of the  $Q$  scans, and the dashed line is the extrapolated background. As the measurements have been performed at constant  $k_f=4.1 \text{ \AA}^{-1}$ , the measured intensity  $I(Q, \omega)$  needs no further correction to yield the magnetic response, and we have

$$I(Q, \omega) \propto S(Q, \omega) \propto \chi''(Q, \omega) / [1 - \exp(-\hbar\omega/k_B T)] \quad (1)$$

and we get  $\chi''$  as reported on Fig. 3(b). Because of the limited resolution, we cannot draw a conclusion on the existence or not of an energy gap below 5 meV. The line shape of  $\chi''$ ,

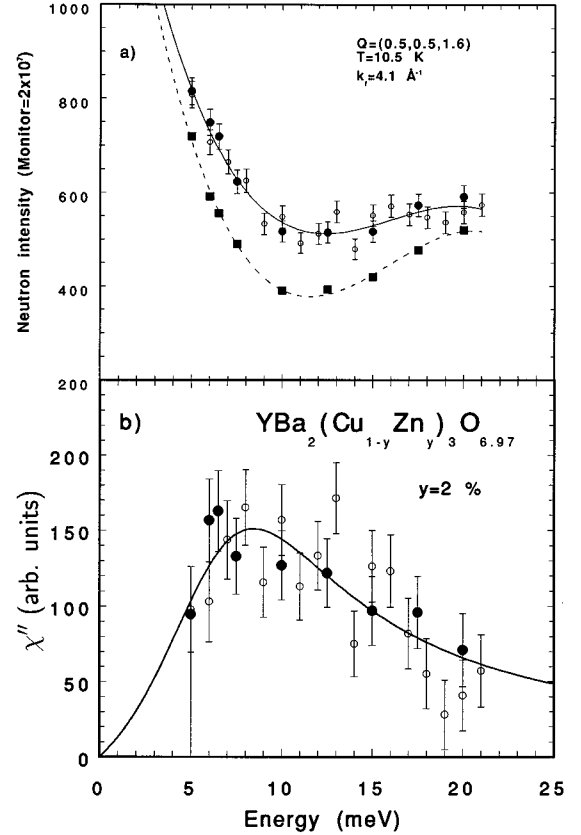


FIG. 3. (a) Energy scan at  $Q_{AF}=(0.5, 0.5, 1.6)$  and  $T=10.5$  K with the PG002 monochromator (open circles). Several  $Q$  scans across the magnetic rod yielded the background (closed squares) and the peak intensity (closed circles). (b)  $\chi''(Q_{AF}, \omega)$  obtained from the difference between the energy scan at  $T=10.5$  K and the estimated background (see text).

with a broad maximum around 9 meV, has been tentatively analyzed as a Lorentzian form, namely  $\chi''(Q_{AF}, \omega) \propto \omega \Gamma / [(\omega - \omega_0)^2 + \Gamma^2]$ , which is used to describe damped excitations. The best fit is obtained for a characteristic energy  $\omega_0=6$  meV and a damping value  $\Gamma=6$  meV. Forcing a pure relaxation, i.e.,  $\omega_0=0$  meV, gives a less satisfactory fit with  $\Gamma=7$  meV. So, zinc substitution induces well defined low energy AF fluctuations whose temperature dependence has been studied.

For that, we have measured the scattered intensity at  $Q_{AF}=(0.5, 0.5, 1.6)$ , and fixed energy transfer  $\hbar\omega=10$  meV with increasing temperature [Fig. 4(a) open circles].  $Q$  scans in the (110) direction have been performed at several temperatures to separate the magnetic signal from the background [Fig. 4(a) closed circles and squares, respectively]. The resulting temperature dependence of  $\chi''$  at  $\hbar\omega=10$  meV—as obtained from the difference between the measured intensity and the interpolated background [dashed line in Fig. 4(a)], and corrected from the temperature factor  $1/[1 - \exp(-\hbar\omega/k_B T)]$ —is shown in Fig. 4(b). The lowering of this correlated intensity upon heating, up to 200 K, is a typical behavior of a magnetic response. But it is noteworthy that the temperature dependence of  $\chi''$  at  $\hbar\omega=10$  meV displays a change when going from the superconducting state to the normal state. Within the accuracy of the measurement, we can see that below  $T_c$   $\chi''$  is almost constant, suggests a

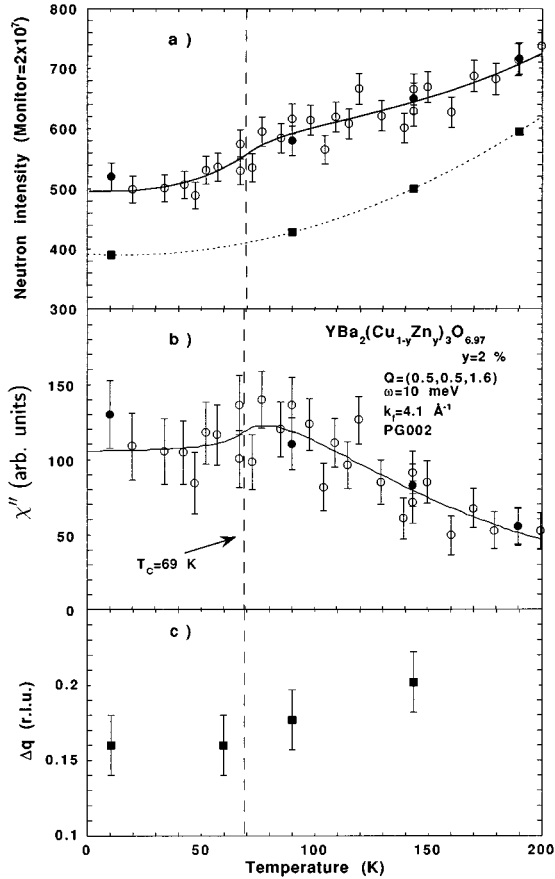


FIG. 4. (a) Temperature dependence of the scattered intensity at  $Q_{AF}=(0.5, 0.5, 1.6)$  and  $\hbar\omega=10$  meV with the PG002 monochromator (open circles). Several  $Q$  scans across the magnetic rod yielded the background (closed squares) and the peak intensity (closed circles). (b)  $\chi''$  temperature dependence at 10 meV obtained from the difference between measured intensity and estimated background [dashed line in (a)]. (c) Temperature dependence of the  $Q$  width (FWHM) deduced from Gaussian fits of  $Q$  scans across the magnetic rod.

possible enhancement around  $T_c$  and a continuous decrease on heating in the normal state.

The  $Q$  scans performed at different temperatures at  $Q_{AF}$  and  $\hbar\omega=10$  meV have been analyzed using a Gaussian line shape as already discussed and illustrated in Fig. 2(a). The deduced  $Q$  width [full width at half maximum (FWHM)] reported in Fig. 4(c) evolves from a low temperature value  $\Delta Q=0.16\pm 0.02$  r.l.u. towards a high temperature value  $\Delta Q=0.20\pm 0.02$  r.l.u. The high temperature value corresponds to that found in the zinc-free YBCO compound in the normal state at the same energy. Therefore the temperature dependence of the  $Q$  width suggests a crossover from zinc induced AF fluctuations at low temperature to AF fluctuations above  $T_c$  similar to those observed in the normal state of zinc-free YBCO. Unfortunately the experimental data are too sparse to ascertain this point.

#### IV. HIGH ENERGY STUDY

Let us now consider the dynamical magnetic susceptibility at higher energy. In the overdoped regime of zinc-free

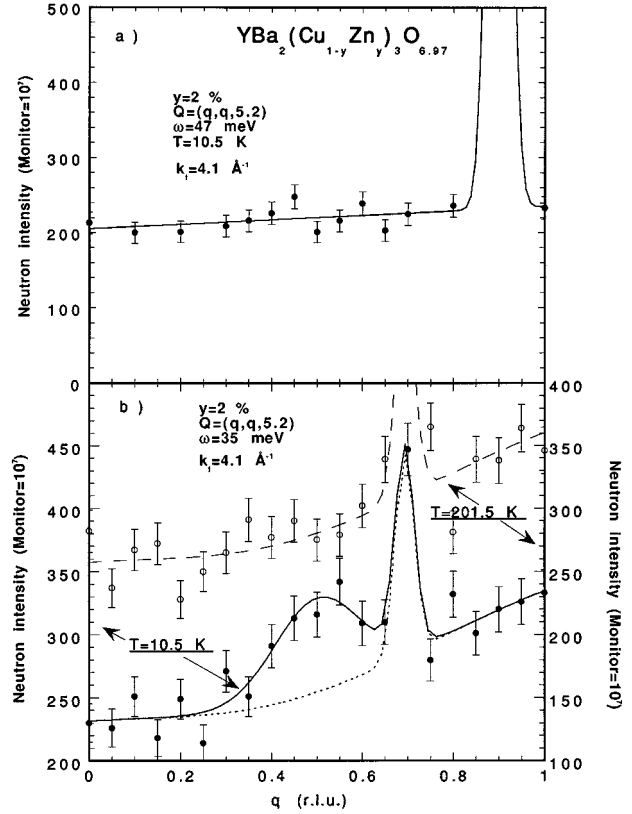


FIG. 5.  $Q$  scans across the magnetic rod at  $q_l=5.2$  and at fixed energy transfer with the Cu111 monochromator: (a)  $\hbar\omega=47$  meV and (b)  $\hbar\omega=35$  meV. Full circles correspond to measurements performed at  $T=10.5$  K and open circles to  $T=201.5$  K. In these measurements the peaks observed, respectively, at  $q=0.9$  r.l.u. and  $q=0.7$  r.l.u. are related to known spurious effects due to some incoherent process on the Cu111 monochromator (Ref. 12). The full line corresponds to a Gaussian centered at  $Q=(0.5, 0.5, 5.2)$  in addition to the background.

YBCO, previous INS measurements pointed out that magnetic fluctuations were located in a narrow energy range,  $\hbar\omega=32-47$  meV.<sup>4,12,14</sup> Investigation at high energies implies measurements at  $Q_{AF}=(0.5, 0.5, 5.2)$  where nuclear scattering becomes a real nuisance. Also extracting the magnetic signal in the high energy range requires caution.<sup>5</sup>

The first step was to perform several  $Q$  scans in the (110) direction around  $Q_{AF}$  using the Cu111 monochromator. For several energy values such  $Q$  scans display a flat or at least slowly varying background on the top of which a magnetic signal peaked at  $Q_{AF}$  eventually appears. Figure 5(a) depicts a  $Q$  scan performed at  $T=10.5$  K in the (110) direction at energy transfer  $\hbar\omega=47$  meV, yielding a nearly constant background. In  $YBa_2Cu_3O_{6.97}$ ,<sup>12</sup>  $\chi''$  is strongly depressed above a ‘‘cutoff energy,’’ located at  $\hbar\omega\approx 47$  meV. Figure 5(a) illustrates that this feature remains upon zinc substitution. On Fig. 5(b) another measurement, performed at  $\hbar\omega=35$  meV for  $T=10.5$  K and  $T=201.5$  K, shows clearly a scattering peaked at  $Q_{AF}$  at low temperature, which vanishes upon heating. Such wave vector and temperature dependences signal the magnetic nature of this intensity. The line shape of this scattering has been analyzed with a Gaussian functional form, yielding, without resolution correction, a  $Q$  width  $\Delta Q$

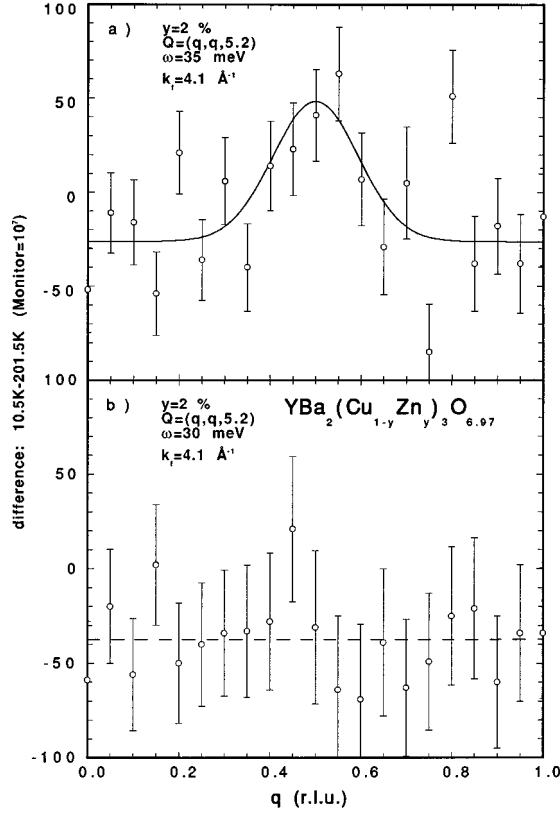


FIG. 6. Difference between  $Q$  scans, performed at  $T=10.5$  K and  $T=201.5$  K, across the magnetic rod at  $q_l=5.2$  and at fixed energy transfer: (a)  $\hbar\omega=35$  meV [raw  $Q$  scans are those of Fig. 5(b)] and (b)  $\hbar\omega=30$  meV (the dashed line corresponds to the average value).

$=0.22 \pm 0.02$  r.l.u. (FWHM). A similar  $q$  dependence characterizes the magnetic fluctuations in zinc-free compound with the same oxygen content at the same energy.<sup>12</sup> In the same time,  $q$  scan along the (001) direction, still performed at  $\hbar\omega=35$  meV and at low temperature, displays a modulation of the intensity which can be reliably ascribed to the usual “acoustic” magnetic structure factor, associated with the  $CuO_2$  bilayer, of the magnetic fluctuations,<sup>12,14</sup> as previously seen at low energy at  $\hbar\omega=10$  meV in Fig. 2(b).

Several nonmagnetic contributions also peaked at  $Q_{AF}$  have already been identified.<sup>5,12</sup> Upon heating, they display only the Bose factor enhancement which is small in the temperature and energy ranges of interest. In contrast, the magnetic fluctuations exhibit a temperature dependence which cannot be ascribed to the Bose factor enhancement, since the magnetic intensity vanishes upon heating [see Fig. 5(b)]. This is why performing the difference between high and low temperatures is an efficient way to extract the magnetic intensity. Figures 6(a) and 6(b) show the differences between  $Q$  scans, performed at  $T=10.5$  K and  $T=201.5$  K, in the (110) direction at the energy transfers  $\hbar\omega=35$  meV and  $\hbar\omega=30$  meV, respectively. In Fig. 6(a), this difference yields a scattering peaked at  $Q_{AF}$  on the top of a nearly constant level which is negative as a consequence of the Bose factor enhancement of the background. On the other hand, in Fig. 6(b), no scattering peaked at  $Q_{AF}$  is observed within error bars. That means that, at low temperature, any signal due to

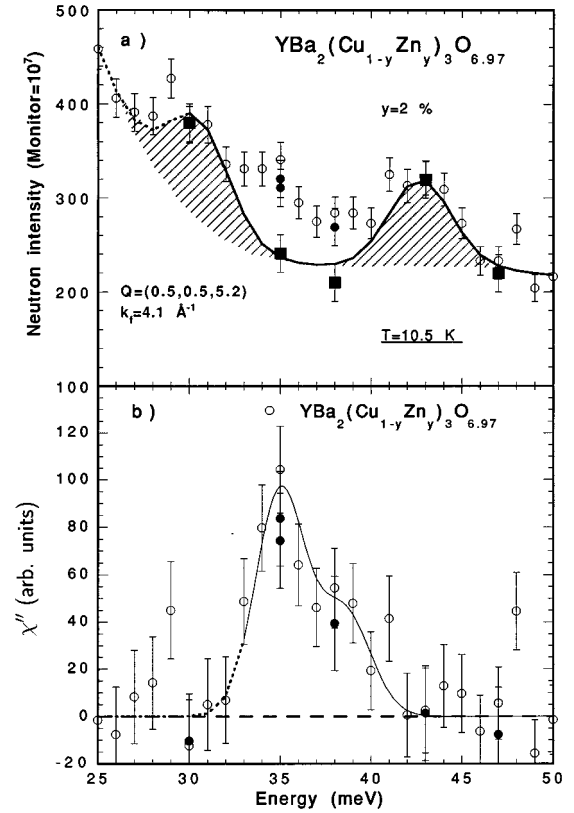


FIG. 7. (a) Energy scan at  $Q_{AF}=(0.5, 0.5, 5.2)$  and  $T=10.5$  K obtained with the Cu111 monochromator (open circles). Several scans across the magnetic rod yielded the background (full squares) and the peak intensity (closed circles) (see text). (b)  $\chi''(Q_{AF}, \omega)$  obtained from the difference between measurement at  $T=10.5$  K and the background described by the solid line in (a). The line is a guide to the eye.

magnetic fluctuations would be smaller than 30 counts at  $\hbar\omega=30$  meV. That points out a clear reduction of magnetic fluctuations as the energy is lowered from  $\hbar\omega=35$  meV to  $\hbar\omega=30$  meV at  $T=10.5$  K. This feature has already been observed in the overdoped regime of zinc-free YBCO.<sup>4,12</sup>

Having ascertained the existence of AF fluctuations at high energy (around  $\hbar\omega=35$  meV), we tried to determine their energy dependence by performing an energy scan at constant  $Q=(0.5, 0.5, 5.2)$  and at  $T=10.5$  K, in the superconducting state [Fig. 7(a)]. The results are reported in Fig. 7(a) and it is clear that the raw data could not be interpreted straightforwardly. To extract the magnetic scattering we need to know the detailed line shape of the background. For that, we have to use what is already known from other measurements. Indeed previous studies on YBCO (Refs. 4, 5, 12) provide a generic background which consists, in this energy range, of a smooth broad nuclear contribution on which are superimposed two well defined nuclear contributions, likely phonons modes,<sup>14</sup> which have a resolution limited linewidth, namely 4.7 meV in the present experimental conditions. Two Gaussian functions  $g(\omega)$ , with that linewidth, respectively, centered at  $\hbar\omega_1=30.5$  meV and  $\hbar\omega_2=42.7$  meV, should account for these nuclear peaks. Furthermore we know that their intensities are in a 1.2 ratio.<sup>12</sup> Therefore, to extrapolate the background, we used the following law:

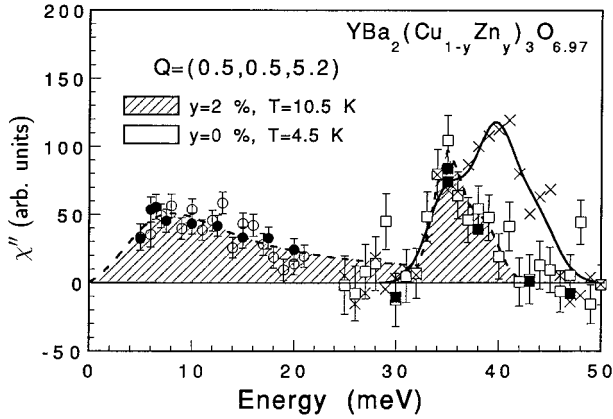


FIG. 8. The complete  $\chi''(Q_{\text{AF}}, \omega)$  curve at  $T=10.5\text{ K}$ , obtained from the combination of Fig. 7(b) (squares) and Fig. 3(b) (circles), normalized as explained in the text. Full symbols correspond to  $Q$  scans performed across the magnetic rod at different energies. The results obtained at  $T=4.5\text{ K}$  in zinc-free compound at the same oxygen content and scaled through a longitudinal phonon measurement are reported for comparison (crosses) (Ref. 12). Both solid and dashed lines are guides to the eye.

$$B_g(\omega) = a + b \exp(-c\omega^2) + d[1.2g(\omega_1) + g(\omega_2)] \quad (2)$$

and we used the  $Q$  scans to determine the  $a, b, c, d$  values. As a consistency check, we have fitted, with the same law, the results obtained in the same conditions on the same sample, but with an oxygen content 6.1, where the magnetic signal was easy to describe in the spin wave formalism. On the other hand, using the scaling factor between samples, we checked the consistency of this background determination on the pure  $\text{YBa}_2\text{Cu}_3\text{O}_{6.97}$  sample.<sup>12</sup> This yielded us a very consistent set of parameters and we think that this procedure guarantees the reliability of the background reported as a continuous line on Fig. 7(a). The main uncertainty is in the range  $\hbar\omega=25\text{--}30\text{ meV}$  [dashed line in Fig. 7(a)]. The  $Q$  scan at  $\hbar\omega=30\text{ meV}$  indicates that there is no sizeable intensity at this energy, but a small signal at lower energy could have been missed due to the extrapolation of the background.

Subtracting the extrapolated background to the measurements gives, after correction from the thermal factor [cf. Eq. (1)], the magnetic response which is reported in Fig. 7(b).

## V. COMPARISON WITH $\text{YBCO}_{6.97}$

In order to have an overview of the whole dynamical magnetic susceptibility, the final step was to scale the low and high energy parts of the magnetic response. This required monitor corrections, bilayer structure factor correction and corrections due to the use of different monochromators. The consistency of these corrections has been checked on measurements at  $\hbar\omega=10\text{ meV}$  and  $T=10.5\text{ K}$  which have been performed in both experimental conditions. The magnetic response is displayed on Fig. 8, together with that of the pure sample.

The main differences between the magnetic responses in the superconducting state of zinc substituted and zinc-free samples are now clearly seen: a magnetic signal appears at low energies, below the spin gap of the pure system, while

the resonance feature vanishes. Nevertheless the situation deserves a more careful examination.

Indeed, it is also obvious on Fig. 8 that the abrupt increase of  $\chi''$  at about  $32\text{ meV}$ , which points out the spin gap in the zinc-free compound, is still present in the zinc substituted one. This point emphasizes that the system retains the memory of the spin gap upon zinc substitution.

Secondly, we have to examine the possibility that the intensity remaining around  $\hbar\omega=35\text{ meV}$  would be due to a renormalization of the resonance feature, observed in the zinc-free compound at  $E_r=39\text{ meV}$ . The main characteristics of the resonance are its temperature dependence and its narrowing in  $q$  space. Indeed in  $\text{YBa}_2\text{Cu}_3\text{O}_{6.97}$ , it vanishes at  $T_c$  and exhibits an intrinsic  $Q$  width ( $\Delta Q=0.26\text{ \AA}^{-1}$ ) twice smaller than at any other energies where AF fluctuations are sizeable ( $\Delta Q=0.45\text{ \AA}^{-1}$ ). In the zinc substituted sample, no marked change occurs at  $T_c$  in the intensity measured at  $\hbar\omega=35\text{ meV}$  and the measurement of the  $Q$  width of the scattering yields a deconvoluted value of  $\Delta Q=0.45\text{ \AA}^{-1}$ , whereas the value is still of  $0.26\text{ \AA}^{-1}$  at  $\hbar\omega=38\text{ meV}$ . On the one hand, this indicates that the maximum at  $\hbar\omega=35\text{ meV}$  is not the renormalized resonance. On the other hand, this also points out that there might be something left of the resonance feature at  $\hbar\omega=38\text{ meV}$ . Unfortunately, the intensity measured at this energy is too weak and this point cannot be definitely ensured. As to the small enhancement of the maximum at  $\hbar\omega=35\text{ meV}$ , it could be simply due to a tiny reduction of the hole doping upon zinc substitution, as we know from zinc-free YBCO that such a reduction should give rise to an increase of  $\chi''$  at this energy. Finally, we would like to emphasize that energy scans in the range  $25\text{--}50\text{ meV}$ , performed at different temperatures, do not show any qualitative differences when going from the superconducting state to the normal state. And this conclusion, which does not depend on data reduction, constitutes one of the major differences induced by the zinc substitution.

## VI. DISCUSSION

First, we would like to summarize some results obtained by various techniques that may be related to our findings. Indeed, among many other works,  $^{89}\text{Y}$  nuclear magnetic resonance (NMR),<sup>2,15</sup>  $^{63}\text{Cu}$  NMR,<sup>16</sup> Mössbauer spectroscopy,<sup>17</sup> have pointed out strong effects due to zinc substitution in YBCO system. Mahajan *et al.*<sup>15</sup> have found indication that a small amount of Cu around Zn exhibits small magnetic moment in the  $\text{CuO}_2$  planes. Ishida *et al.*<sup>16</sup> came to the conclusion that in zinc substituted  $\text{YBa}_2\text{Cu}_3\text{O}_7$  there exists a finite electronic density of states (DOS) at the Fermi level in the superconducting state. This was suggested by the temperature and the zinc content dependences of  $^{63}\text{Cu}$  Knight shift and nuclear spin relaxation rate,  $T_1$ , and is in agreement with Mössbauer spectroscopy,<sup>17</sup> specific heat measurements,<sup>18</sup> and  $\text{Gd}^{3+}$  electronic spin resonance.<sup>19</sup> These results may be accounted for by the theory, either when nonmagnetic impurities are treated in the unitary limit for an anisotropic superconducting order parameter,<sup>20</sup> or when magnetic pair breaking occurs due to local moments around zinc sites.<sup>3,15</sup> In addition to finite DOS at the Fermi level, the lifetime of the quasiparticles involved in the superconducting pairing mechanism must be strongly lowered.<sup>21</sup> Finally, Ishida *et al.*<sup>16</sup> have also shown the existence of two

relaxation times ascribed to  $^{63}\text{Cu}$  sites away from and near zinc impurities.

Our measurements in the low energy range of  $\chi''$  are clearly related to such peculiarities of the zinc substituted YBCO system. The appearance of a magnetic response in the superconducting state directly reflects the appearance of a finite DOS at the Fermi level, which provides possible magnetic fluctuations. The temperature dependence of  $\chi''$  at  $\hbar\omega=10$  meV, as reported on Fig. 4(b), displays some significant features: a possible enhancement around  $T_c$  and an evolution of the  $Q$  width from a low temperature value of 0.16 r.l.u. up to a value of 0.20 r.l.u. above  $T_c$ , which is that found in the pure system. This is strongly in favor of the coexistence of two contributions to the magnetic response, one seen at low temperature and nearly unaffected by the superconductivity, the second one appearing above  $T_c$  and displaying the same behavior as in the pure system. This overall temperature dependence at low energy is consistent with the report by Ishida *et al.*<sup>16</sup> of two relaxation times in the measurements of the  $^{63}\text{Cu}$  nuclear spin relaxation rate,  $T_1$ , even though the relative magnitude of the two contributions cannot be obtained. Finally, we may point out that the low temperature  $Q$  width corresponds to a characteristic length of 7 Å, which is an estimated range of the perturbation induced by zinc impurities still isolated for this kind of zinc content.<sup>19</sup>

At this stage, our INS results also suggest the picture of  $\text{CuO}_2$  planes where zinc impurities induce some perturbation on a range of about 7 Å giving rise to two different kinds of Cu sites.

Turning now to the high energy part of  $\chi''$ , the main effect of the zinc substitution is the strong variation of the resonance feature. As this resonance is strongly correlated to the superconductivity in the pure system, such a drastic effect is not unexpected according to the strong reduction of  $T_c$  for a low zinc substitution. But, to try to understand the origin of this effect, we need the help of the theoretical approaches, which are able to account for this unusual feature in the pure system. Among others, the model developed by Onufrieva *et al.*<sup>7</sup> provides some consistent picture of this behavior. Using diagrammatic techniques for Hubbard operators in the framework of the  $t$ - $t'$ - $J$  model, this approach gives a formulation of  $\chi''$  as a combination of two contributions. The first arises from the subsystem of itinerant charge carriers. The second corresponds to the localized spins subsystem with short range AF correlations related to two spinon spectral function. In the pure system the respective evolutions of these two contributions with hole doping allows us to account for the experimental observations quite satisfactorily. In this model the resonance peak arises from the itinerant contribution in the presence of superconductivity and van-

ishes in the normal state. Other models,<sup>22</sup> even though they handle different concepts, explain the resonance peak as due to spin-flip electron excitations across the superconducting gap with an enhancement of the susceptibility due to the antiferromagnetic interaction between Cu spins. We see that these kinds of models provide us with the necessary ingredients for a qualitative discussion of our observations. Indeed, the existence of the low energy part of  $\chi''$  and the results of NMR measurements clearly indicates that zinc substitution affects some of the Cu sites, either by slightly reinforcing the localized character or more effectively by reducing the lifetime of the quasiparticles involved in the superconducting mechanism.<sup>21</sup> In the above-mentioned approaches, the alteration of the itinerant character must induce a strong effect on the resonance, in agreement with our observations.

## VII. CONCLUSION

In  $\text{YBa}_2(\text{Cu}_{1-y}\text{Zn}_y)_3\text{O}_{6.97}$ , the imaginary part of the dynamical susceptibility,  $\chi''$ , is markedly different from that of the pure system. Main differences appear in the low energy range where a broad contribution is found around  $\hbar\omega\approx 9$  meV and in the high energy range where a maximum is observed around 35 meV, but without the characteristics of the resonance observed in the pure system. Nevertheless a careful examination of the energy and temperature dependences of  $\chi''$  allows the conclusion that the zinc substituted system retains the memory of the spin gap, still defined by the inflection point in the  $\chi''$  curve at  $E_G=33$  meV. The coexistence of a low energy signal with this gaplike feature could be related to the existence of two kinds of copper sites, the spin gap being then related to zinc-independent hole density in  $\text{CuO}_2$  planes. These results are consistent with the existence of a finite DOS at the Fermi level,<sup>16-18</sup> and with NMR findings of two relaxation times.<sup>16</sup> Likewise, the resonance feature, which is known to be closely related to superconductivity, is strongly reduced upon zinc substitution, even if there remains some hint of it. This could be understood as resulting from the modification induced by the zinc substitution essentially to the itinerant contribution to the magnetic response. This is likely the more prominent feature regarding the drastic effect induced on superconductivity by zinc substitution. We hope that the present results will help to develop further theoretical and experimental investigations to progress in the understanding of the superconducting properties of high- $T_c$  cuprates.

## ACKNOWLEDGMENTS

We wish to acknowledge M. Braden for his assistance during experiment. Discussions with F. Onufrieva, H. Alloul, P. Mendels, P. Pfeuty, and S. Aubry have been appreciated.

<sup>1</sup>G. Xiao, M. Z. Cieplak, A. Gravin, F. H. Streitz, A. Bahashai, and C. L. Chien, *Phys. Rev. Lett.* **60**, 1446 (1988).

<sup>2</sup>H. Alloul, P. Mendels, H. Casalta, J. F. Marucco, and J. Arabiski, *Phys. Rev. Lett.* **67**, 3140 (1991).

<sup>3</sup>A. Abrikosov, *Fundamental of the Theory of Metals* (North-Holland, Amsterdam, 1989).

<sup>4</sup>L. P. Regnault, P. Bourges, P. Burlet, J. Y. Henry, J. Rossat-Mignod, Y. Sidis, and C. Vettier, *Physica C* **235-240**, 59 (1994), and references therein.

<sup>5</sup>P. Bourges, L. P. Regnault, J. Y. Henry, C. Vettier, Y. Sidis, and P. Burlet, *Physica B* **215**, 30 (1995).

<sup>6</sup>H. A. Mook, Y. Yethiraj, G. Aeppli, T. E. Mason, and T. Arm-

- strong, Phys. Rev. Lett. **70**, 3490 (1993).
- <sup>7</sup>F. Onufrieva and J. Rossat-Mignod, Physica C **235–240**, 1687 (1994); Phys. Rev. B **52**, 7572 (1995).
- <sup>8</sup>K. Kakurai, S. Shamoto, T. Kiyokura, M. Sato, J. M. Tranquada, and G. Shirane, Phys. Rev. B **48**, 3485 (1993).
- <sup>9</sup>P. Bourges, Y. Sidis, B. Hennion, R. Villeneuve, G. Collin, and J. F. Marucco, Physica C **235–240**, 1683 (1994).
- <sup>10</sup>H. Harashina, S. Shamoto, T. Kiyokura, M. Sato, K. Kakurai, and G. Shirane, J. Phys. Soc. Jpn. **62**, 4009 (1993).
- <sup>11</sup>Y. Sidis, P. Bourges, B. Hennion, R. Villeneuve, G. Collin, and J. F. Marucco, Physica C **235–240**, 1591 (1994).
- <sup>12</sup>P. Bourges, L. P. Regnault, Y. Sidis, and C. Vettier, Phys. Rev. B **53**, 876 (1996).
- <sup>13</sup>L. Pintschovius, Nucl. Instrum. Methods Phys. Res. A **338**, 136 (1994).
- <sup>14</sup>H. F. Fong, B. Keimer, P. W. Anderson, D. Reznik, F. Dogan, and I. A. Aksay, Phys. Rev. Lett. **75**, 316 (1995).
- <sup>15</sup>V. A. Mahajan, H. Alloul, G. Collin, and J. F. Marucco, Phys. Rev. Lett. **72**, 3100 (1994).
- <sup>16</sup>K. Ishida, Y. Kitaoka, N. Ogata, T. Kamino, K. Asayama, J. R. Cooper, and N. Athanassopoulou, J. Phys. Soc. Jpn. **62**, 2803 (1993).
- <sup>17</sup>J. A. Hodges, P. Bonville, P. Imbert, and A. Pinatel-Philippot, Physica C **246**, 323 (1995).
- <sup>18</sup>J. W. Loram, K. A. Mirza, and P. F. Freeman, Physica C **171**, 243 (1990).
- <sup>19</sup>A. Janossy, J. R. Cooper, L. C. Brunel, and A. Carrington, Phys. Rev. B **50**, 3445 (1994).
- <sup>20</sup>T. Hotta, J. Phys. Soc. Jpn. **62**, 274 (1993), and references therein.
- <sup>21</sup>A. V. Balatsky, P. Monthoux, and D. Pines, Phys. Rev. B **50**, 582 (1994).
- <sup>22</sup>I. I. Mazin and V. M. Yakovenko, Phys. Rev. Lett. **75**, 4134 (1995); D. Z. Liu, Y. Zha, and K. Levin, *ibid.* **75**, 4130 (1995); F. Onufrieva, Physica C **251**, 348 (1995).